JOURNAL OF PROPULSION AND POWER
Vol. 12, No. 1, January–February 1996

Technical Notes

TECHNICAL NOTES are short manuscripts describing new developments or important results of a preliminary nature. These Notes cannot exceed 6 manuscript pages and 3 figures; a page of text may be substituted for a figure and vice versa. After informal review by the editors, they may be published within a few months of the date of receipt. Style requirements are the same as for regular contributions (see inside back cover).

Optimal Shock Wave Parameters for Supersonic Inlets

Pavel Safarik*
Czech Technical University, 16607 Prague, Czech Republic
and
Arnold Polak†
University of Cincinnati, Cincinnati, Ohio 45221

Nomenclature

M	=	Mach number
n	=	total number of shock waves in the system
p, p_0	=	static, stagnation pressure
S	=	ratio of the overall total pressure ratio for an n-shock-wave system to the total pressure ratio for case with a single shock
β	=	shock-wave inclination
δ	=	flow deflection
ξ_i	=	ratio of static pressures, p_{i+1}/p_i

Subscripts

$i(1, 2, \ldots, n)$	=	number of the shock in the system
j, k	=	number of iteration step
∞	=	limiting value for $n \to \infty$

Introduction

THE effectiveness of supersonic inlets is strongly influenced by the unavoidable presence of shock waves. At high supersonic speeds it is desirable to design inlets with multiple-shock configuration in order to maximize the pressure recovery. The theory of shock waves is based on the assumption of discontinuity in flow parameters across the shock surface and the requirement that the principles of conservation of mass, momentum, and energy across this surface be satisfied. This approach results in shock relations, which when combined with a pressure recovery criteria, yields values of the shock parameters corresponding to the optimal shock configuration. In the principal work by Oswatitsch[1] the optimization problem is formulated for n-shock-wave system $n - 1$ of these being oblique shocks and the last one a normal shock wave. The task set forth is to determine, for a given n and an upstream Mach number M_1, the shock configuration producing the maximum overall total pressure ratio p_{0n+1}/p_{01}. The solution to this problem yields δ_i. It is possible to formulate the optimization problem for n oblique shock waves by specifying M_1 and the ratio of static pressures p_{n+1}/p_1, or specify M_1 and M_{n+1}. As long as $M_{n+1} \leq 1.3$ the additional loss in total pressure due to deceleration from M_{n+1} to subsonic speed would be very small. Other choices also exist. In this Note a number of optimization problems for a system of two or more shock waves will be formulated. The optimization criterion in all of these problems is that the overall ratio of total pressures be maximum.

Received Nov. 1, 1993; revision received March 15, 1995; accepted for publication March 30, 1995.

*Research Specialist, Faculty of Mechanical Engineering, Department of Fluid Mechanics and Thermodynamics.

†Professor, Department of Aerospace Engineering and Engineering Mechanics. Associate Fellow AIAA.

Formulation of the Problem

The two-dimensional flow geometry together with pertinent parameters to be considered in the present analysis is exhibited in Fig. 1. The following optimization tasks will be considered: 1) p_3/p_1 and M_1 are specified, 2) M_1 and M_3 are specified, and 3) δ_1 and δ_2 are specified. In all of these cases the criterion p_{03}/p_{01} = max will be imposed. All remaining flow parameters will be solved for.

Solution of the Optimization Task

In the analysis that follows we shall assume the fluid to be an inviscid perfect gas with a ratio of specific heats equal to 1.4. Substituting the oblique shock relation[2]

$$\frac{p_{0i+1}}{p_{0i}} = \left(\frac{6\xi_i + 1}{\xi_i + 6}\right)^{7/2} \xi_i^{-5/2} \tag{1}$$

into the identity

$$\frac{p_{03}}{p_{01}} = \frac{p_{03}}{p_{02}}\frac{p_{02}}{p_{01}} \tag{2}$$

and using the optimization criterion $\mathrm{d}(p_{03}/p_{01}) = 0$ we obtain

$$\frac{\mathrm{d}\xi_2}{\mathrm{d}\xi_1} = -\left(\frac{\xi_1 - 1}{\xi_2 - 1}\right)^2 \frac{\xi_2}{\xi_1}\frac{6\xi_2 + 1}{6\xi_1 + 1}\frac{\xi_2 + 6}{\xi_1 + 6} \tag{3}$$

This equation has to be satisfied for any of the optimization tasks proposed previously.

Case a: Given p_3/p_1 and M_1

At the outset it must be realized that for any given value of p_3/p_1, a lower limit for M_1 exists. This limiting value will

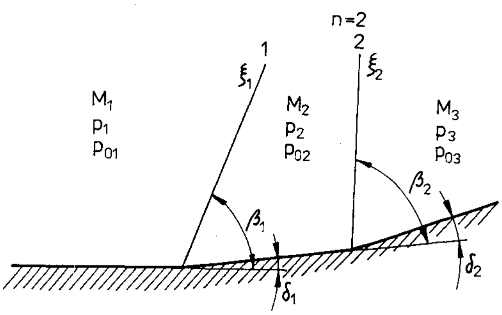

Fig. 1 Flow and shock wave geometry.

be ascertained later. Independently of the value of M_1, from $p_3/p_1 = \xi_1\xi_2 = \text{const}$, it follows:

$$\frac{d\xi_2}{d\xi_1} = -\frac{\xi_2}{\xi_1} \tag{4}$$

Combining Eqs. (3) and (4) we obtain

$$\left(\frac{\xi_1 - 1}{\xi_2 - 1}\right)^2 \frac{6\xi_2 + 1}{6\xi_1 + 1}\frac{\xi_2 + 6}{\xi_1 + 6} = 1 \tag{5}$$

which is valid only when

$$\xi_1 = \xi_2 = \xi = \sqrt{p_3/p_1} \tag{6}$$

This result is identical to Oswatitsch's solution. The remaining flow parameters are now obtained:

Flow deflection after the first and the second wave:

$$\delta_i = \arctan\left[\frac{5(\xi - 1)}{7M_i^2 - 5(\xi - 1)}\sqrt{\frac{7M_i^2}{6\xi + 1} - 1}\right] \tag{7}$$

Inclinations of the first and the second wave:

$$\beta_i = \arcsin\sqrt{(6\xi + 1)/7M_i^2} \tag{8}$$

Mach numbers after the first and the second wave:

$$M_{i+1} = \sqrt{\frac{M_i^2(6\xi + 1) - 5(\xi^2 - 1)}{\xi(\xi + 6)}} \tag{9}$$

where $i = 1, 2$. The optimal value for the ratio of total pressures is obtained from Eqs. (1) and (6):

$$\frac{p_{03}}{p_{01}} = \left(\frac{6\xi + 1}{\xi + 6}\right)^7 \xi^{-5} \tag{10}$$

The choice of p_3/p_1 and M_1 must be controlled by the limiting case, that of the second wave being a normal shock. With the limiting value $\beta_2 = \pi/2$, Eq. (8) is satisfied for

$$M_2 = \sqrt{(6\xi + 1)/7} \tag{11}$$

Entering with this value of M_2 the Eq. (9), the lower bound of M_1 is determined for a given value of p_3/p_1:

$$M_{1\,\text{min}} = \sqrt{\frac{\xi(\xi + 6)}{7} + \frac{5(\xi^2 - 1)}{6\xi + 1}} \tag{12}$$

A sample calculation with $p_3/p_1 = \xi^2 = 16$ and $M_1 = 3.50$ yields the following values for the pertinent flow parameters: $\delta_1 = 18.29$ deg, $\delta_2 = 24.86$ deg, $M_2 = 2.40$, $M_3 = 1.32$, and $p_{03}/p_{01} = 0.60$.

Case b: Optimization Task for Given M_1 and M_3

Equation (9) is used to obtain M_2^2 in terms of M_1^2 and M_3^2:

$$M_2^2 = \frac{(M_1^2 + 5)(6\xi_1 + 1)}{\xi_1(\xi_1 + 6)} - 5 \tag{13}$$

$$M_2^2 = \frac{(M_3^2 + 5)\xi_2(\xi_2 + 6)}{6\xi_2 + 1} - 5 \tag{14}$$

Differentiating Eqs. (13) and (14) with respect to ξ_1 and ξ_2, respectively, while holding M_1 and M_3 constant, and combining these two results will produce

$$\frac{d\xi_2}{d\xi_1} = -\frac{M_1^2 + 5}{M_3^2 + 5}\frac{(3\xi_1^2 + \xi_1 + 3)(6\xi_2 + 1)^2}{\xi_1^2(\xi_1 + 6)^2(3\xi_2^2 + \xi_2 + 3)} \tag{15}$$

The desired expression for $d\xi_2/d\xi_1$, in terms of ξ_1 and ξ_2 only, will be obtained after eliminating the ratio $(M_1^2 + 5)/(M_3^2 + 5)$ from Eq. (15). This ratio is determined from Eqs. (13) and (14):

$$\frac{M_1^2 + 5}{M_3^2 + 5} = \xi_1\xi_2\frac{(\xi_1 + 6)(\xi_2 + 6)}{(6\xi_1 + 1)(6\xi_2 + 1)} \tag{16}$$

so that

$$\frac{d\xi_2}{d\xi_1} = -\frac{(3\xi_1^2 + \xi_1 + 3)\xi_2(\xi_2 + 6)(6\xi_2 + 1)}{(3\xi_2^2 + \xi_2 + 3)\xi_1(\xi_1 + 6)(6\xi_1 + 1)} \tag{17}$$

Invoking the optimization criterion expressed through Eq. (3) results in

$$\frac{(\xi_1 - 1)^2}{(\xi_2 - 1)^2} = \frac{3\xi_1^2 + \xi_1 + 3}{3\xi_2^2 + \xi_2 + 3} \tag{18}$$

This again is only valid when Eq. (6) is satisfied, i.e., when $\xi_1 = \xi_2 = \xi$. The value of ξ, in terms of M_1 and M_3, is now determined from Eq. (16) by setting $\xi_1 = \xi_2 = \xi$:

$$\xi = 3(P_s - 1) + \sqrt{9(P_s - 1)^2 + P_s} \tag{19}$$

where

$$P_s = \sqrt{(M_1^2 + 5)/(M_3^2 + 5)}$$

It must be emphasized that even though Eq. (6) is valid in both cases a and b, these are two different optimization problems. Indeed, if we choose in case b $M_1 = 3.50$ and $M_3 = 1.32$, we obtain from Eqs. (19) and (10) values $\xi = 3.03$ and $p_{03}/p_{01} = 0.76$, respectively. These values are quite different from those obtained earlier in the sample calculation for case a.

Equation (19) can be generalized to multiple wave system $n \geq 2$ by setting

$$\xi = \xi_1 = \xi_2 = \cdots = \xi_n \tag{20}$$

and defining

$$P_s \equiv \sqrt[n]{\frac{M_1^2 + 5}{M_{n+1}^2 + 5}} \tag{21}$$

We can express the ratio of total pressures as a function of the parameter P_s and n

$$p_{0n+1}/p_{01} = (\xi/P_s^{7/2})^n \tag{22}$$

where ξ, according to Eq. (19), is a function of P_s. The advantage of multiple wave system ($n > 1$) can be verified from the ratio p_{0n+1}/p_{01} to single wave case $(p_{02}p_{01})_{n=1}$:

$$S \equiv \frac{p_{0n+1}/p_{01}}{(p_{02}/p_{01})_{n=1}} = \frac{[3(P_s - 1) + \sqrt{9(P_s - 1)^2 + P_s}]^n}{3(P_s^n - 1) + \sqrt{9(P_s^n - 1)^2 + P_s^n}} \tag{23}$$

It is shown in Fig. 2. For $n \to \infty$, the ratio of total pressures in Eq. (22) yields $p_{0\infty}/p_{01} = 1$ and the ratio given by Eq. (23) approaches the value

$$S_\infty = \tilde{P}_s^{7/2}/[3(\tilde{P}_s - 1) + \sqrt{9(\tilde{P}_s - 1)^2 + \tilde{P}_s}]$$

where $\tilde{P}_s = (M_1^2 + 5)/(M_\infty^2 + 5)$. Here, M_∞ denotes the given Mach number after the last wave. The values of S_∞ are

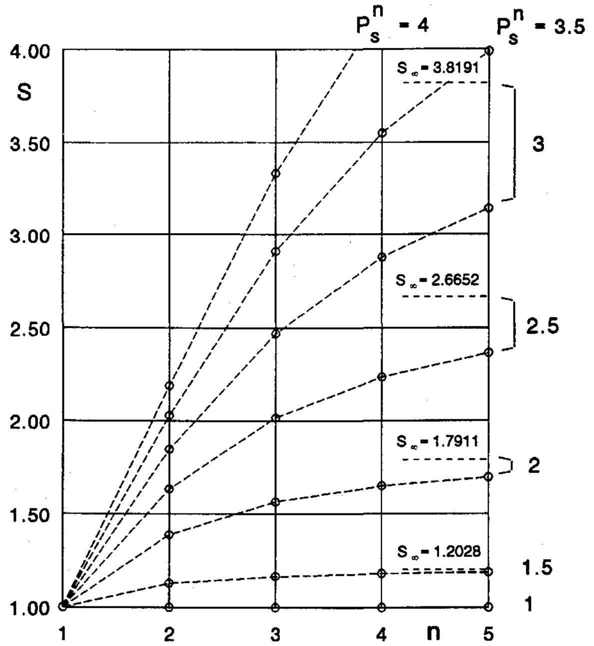

Fig. 2 Effectivity of optimal multiple-shock configuration.

shown in Fig. 2 as well. Lower bound of M_1 is determined for given values of M_1 and M_{n+1} from

$$M_{1\min} = \sqrt{\tfrac{6}{7}[3(P_s + 1) + \sqrt{9(P_s - 1)^2 + P_s}]P_s^{n-1} - 5} \tag{24}$$

Case c: Optimization Task for Given δ_1 and δ_2

This case is applicable when the inlet geometry is given and the optimal parameters, including the freestream M_1 are to be determined. Equation (7) is written here for $i = 1$ or 2 as

$$\tan \delta_i = \left[\frac{5(\xi_i - 1)}{6\xi_i - 1} \bigg/ \frac{7M_i^2}{6\xi_i + 1} - \frac{5(\xi_i - 1)}{6\xi_i + 1}\right] \sqrt{\frac{7M_i}{6\xi_i + 1} - 1} \tag{25}$$

Denoting

$$B_i^2 \equiv \frac{7M_i^2}{6\xi_i + 1} - 1 \tag{26}$$

$$R_i \equiv \frac{5(\xi_i - 1)}{6\xi_i + 1} \tag{27}$$

and using these definitions, Eq. (25) can be rewritten as

$$B_i^2 - \frac{R_i}{\tan \delta_i} B_i + (1 - R_i) = 0 \tag{28}$$

Solving for B_i results in

$$B_i = \frac{R_i}{2 \tan \delta_i} \pm \sqrt{\frac{R_i^2}{4 \tan \delta_i} + R_i - 1} \tag{29}$$

The plus sign corresponds to strong shock solution and the minus sign to weak shock solution. From the standpoint of the optimization task it is desirable to have the first wave to be a weak one and the second to be a strong wave. It can be verified that the discriminant $D_1 = (R_1^2/4 \tan \delta_1) + R_1 - 1$, appearing in the Eq. (29) under the radical sign, vanishes for the special case $\delta_2 = 0$ and $\xi_2 = 1$. This becomes a special case of the optimization problem with a single wave when δ_1 is given. Using the relation (26) to replace M_1^2 and M_2^2 in Eq. (13) results in

$$\left[\frac{(B_1^2 + 1)(6\xi_1 + 1)}{35} + 1\right] \frac{6\xi_1 + 1}{\xi_1(\xi_1 + 6)} = \frac{(B_2^2 + 1)(6\xi_2 + 1)}{35} + 1 \tag{30}$$

From Eq. (28) it is evident that for given δ_1 and δ_2 the parameters B_1 and B_2 are functions of ξ_1 and ξ_2, respectively. Equation (30) is one of the two equations needed to solve for ξ_1 and ξ_2. The second equation to be employed is the Eq. (3) based on the optimization criterion. These equations must be solved numerically. Because of limited space only the key steps used in this numerical solution are given here. We denote the left- and right-hand side of Eq. (30) by F_1 and F_2, respectively:

$$F_1(\xi_1) \equiv \left[\frac{(B_1^2 + 1)(6\xi_1 + 1)}{35} + 1\right] \frac{6\xi_1 + 1}{\xi_1(\xi_1 + 6)} \tag{31}$$

$$F_2(\xi_2) \equiv \frac{(B_2^2 + 1)(6\xi_2 + 1)}{35} + 1 \tag{32}$$

Then we rewrite Eq. (3) as

$$G \equiv \frac{(\xi_2 - 1)^2}{(\xi_1 - 1)^2} \frac{\xi_1}{\xi_2} \frac{(\xi_1 + 6)(6\xi_1 + 1)}{(\xi_2 + 6)(6\xi_2 + 1)} \frac{dF_1}{dF_2} \frac{d\xi_2}{d\xi_1} = -1 \tag{33}$$

The coupled set of Eqs. (30) and (33) is solved by a double-iteration procedure. For a given δ_1 and δ_2 a particular set of initial value $(\xi_1)_0$ and $(\xi_2)_0$ are chosen corresponding to the case $D_1 = 0$. In the first iteration we solve

$$(\xi_1)_j = \frac{(F_1)_{j-1}}{(F_2)_{j-1}} (\xi_1)_{j-1} \tag{34}$$

until $|(\xi_1)_j - (\xi_1)_{j-1}| < 1 \times 10^{-6}$. Then, in the second iteration

$$(\xi_2)_k = G_{k-1}(\xi_2)_{k-1} \tag{35}$$

is solved and in each kth step the iteration procedure (34) for $(\xi_1)_k$ is repeated. The second iteration given by Eq. (35) is repeated until $|(\xi_2)_k - (\xi_2)_{k-1}| < 1 \times 10^{-6}$. Results from such a calculation, corresponding to the sample problem presented for case a, with $\delta_1 = 18.29$ deg and $\delta_2 = 24.86$ deg for the strong second wave [cf., Eq. (29)] are $\xi_1 = 3.48$, $\xi_2 = 3.05$, and $p_{03}/p_{01} = 0.62$.

Concluding Remarks

The optimization tasks considered in this Note, all using the same optimization criterion, produced substantially different results. According to the sample calculations presented herein, for the same values of M_1 and M_3, the corresponding values of p_3/p_1 and p_{03}/p_{01} are quite different in case b from that in case a. Similarly, differences appear also between case a and case c for the same values of δ_1 and δ_2.

Even though most of the details in these analyses were presented for a system of two waves, for case b it was shown how these results can be extended to $n > 2$. Similarly, for case a the extension is easily applied by using Eq. (20). For case c the solution of the optimization task for $n > 2$ is more complex, but can be realized.

References

[1]Oswatitsch, K., "Pressure Recovery for Missiles with Reaction Propulsion at High Supersonic Speeds (The Efficiency of Shock Dif-

fusers)," NACA TM-1140, June 1947.
[2]Ames Research Staff, "Equations, Tables, and Charts for Compressible Flow," NACA Rept. 1135, 1953.

Advanced Instrumentation for Next-Generation Aerospace Propulsion Control Systems

S. Barkhoudarian* and G. S. Cross†
Rockwell International Corporation, Canoga Park, California 91303
and
Carl F. Lorenzo‡
NASA Lewis Research Center, Cleveland, Ohio 44135

Introduction

NEW concepts for the control of jet and rocket engines and the new hybrid engines, such as the National Aerospace Plane (NASP) hypersonic propulsion system, have introduced new instrumentation requirements. These control concepts are analyzed to determine their required measurands. Next, advanced measurement technologies from recent major NASA/Department of Defense (DOD)/industry-sponsored measurement technology development programs are compiled and, subsequently, matched with the corresponding measurands. This is followed by a ranking of the sensor technologies based on the number of their applications. This provides a list of advanced measurement technologies suggested for further development and use in advanced aerospace propulsion control systems.[1]

Control Concepts

Jet Engines

Several new concepts for the control of jet and turbofan engines have been forwarded in recent years. These ideas include active stall control, performance-seeking control, intelligent diagnostic control, tip clearance control, burner pattern-factor control, control of the normal shock in the inlets of supersonic and hypersonic aircraft, acoustic emissions control, and electromagnetic emissions control. Intelligent control concepts for jet engines encompass the management of a variety of special-purpose control modes such as those just listed, the use of reduced redundancy, and the incorporation of diagnostics and damage reconfiguration.

Rocket Engines

The emergence of the Space Shuttle main engine (SSME) as the world's first reusable rocket engine has brought about a growing interest in improving durability through new control concepts. New rocket-engine control concepts, include onboard diagnostic systems, which will monitor and interpret the health of the rocket engine and provide a real-time prognosis of wear characterization. This information is then used by a higher-level coordinator to either change the control requirements for the rocket engine or to actually change or implement the appropriate control modes of the rocket engine. The underlying idea is to use the engine in a manner that reduces component loads and minimizes the damage that accrues while still ensuring, if possible, mission success. It also requires appropriate advanced instrumentation to either measure damage directly or to measure the damage-indicating parameters such as stress/strain cycles and temperature transients.

Hypersonic Engines

Combined-cycle engines are characterized by the presence of high-speed flow in excess of Mach 1 through the entire engine. A controller for this system would also have to handle ramjet engines that can be transitioned into scramjet engines, the management of shocks, and the control of combustion under extremely adverse conditions.

Emerging Instrumentation Technologies

The recent NASA/DOD integrated high-performance turbine engine technology (IHPTET) initiative has become a driving force in the design of control systems and the development of advanced instrumentation for jet-engine propulsion systems.

Furthermore, the NASA-LeRC rocket engine maintenance study program has identified and developed several advanced measurement technologies for in-flight and between-flight hardware diagnosis and intelligent control of rocket engines. They were fiberoptic pyrometers for very high-speed blade-by-blade temperature mapping for the detection of blade fatigue cracks, fiberoptic deflectometers for hf deflection measurement for ball-bearing health-monitoring purposes and isotope wear indicators for nonintrusively monitoring the wear of parts (ball bearings, blade tips) in situ without access ports or holes.

Other major advanced instrumentation programs are the NASA Marshall SSME technology testbed engine program and the NASA Lewis multipoint multiparameter hypersonic combustion flow diagnostic system, which included remote optical monitoring of the two-dimensional distribution of the temperature, pressure, and concentration of various species simultaneously superimposed on top of each other.

Another major effort was performed by the NASP instrumentation consortium. The consortium generated a list of 22 measursands desirable for the monitoring and control of NASP hypersonic engines and initiated the development of 10 advanced measurement technologies.

Application of Emerging Instrumentation Technologies to New Control Concepts

To determine the application of the identified advanced measurement technologies to the new control concept, they were matched against the new control-concept measurands for jet, rocket, and hypersonic engines. Only new technologies that provide measurements not previously available are discussed further. This includes sensor technologies that provide increased dimensionality of measurements. Nonintrusive measurements are also included since they permit measurements in areas where conventional probe instrumentation cannot be used or reduce the number of ports required. The technologies must have the near-term potential to be flyable, implying that they must be lightweight, robust, and require a minimal amount of electrical power. In many instances, being robust means the capability of operating in extreme high-temperature environments.

Table 1 shows a ranking of selected technologies based on the combined number of applications for jet, rocket, and

Presented as Paper 93-2079 at the AIAA/SAE/ASME/ASEE 29th Joint Propulsion Conference and Exhibit, Monterey, CA, June 28–30, 1993; received Dec. 2, 1993; revision received March 1, 1995; accepted for publication May 30, 1995.

*Manager, Advanced Measurements, Rocketdyne Division. Senior Member AIAA.
†Technical Staff, Advanced Measurements, Rocketdyne Division.
‡Chief Engineer, Instrumentation and Controls Technology Division.